EVS27
Barcelona, Spain, November 17 - 20, 2013

Impact of Current Ripple on Li-ion Battery Ageing

Sven De Breucker[1], Kristof Engelen[2], Reinhilde D'hulst[1] and Johan Driesen[2]
[1]*VITO, Boeretang 200, 2400 Mol, Belgium, sven.debreucker@vito.be*
[2]*EnergyVille, Dennenstraat 7, 3600 Genk, Belgium, johan.driesen@esat.kuleuven.be*

Abstract

The aim of this paper is to investigate the impact of the current ripple, originating from the dc-dc converter of e.g. a PHEV powertrain, on the ageing of Li-ion batteries. Most research concerning batteries focuses on very low (μHz) to low (Hz) frequencies and low current ripples to create very accurate battery models which can determine e.g. the State of Charge of the battery. On the other hand the design of dc-dc converters tries to reduce the current ripple by using multiple phases with interleaving technique and capacitors in parallel with the battery. The interaction between the current ripple of the dc-dc converter and the battery has received little attention so far. A test set-up is build with two identical 304 V, 12 kWh Li-ion batteries and two 100 A dc-dc converters. The dc-dc converter can be connected to an LCL-filter or solely to the primary inductor of this filter, such that the battery current contains a small or large current ripple respectively. The batteries are discharged and charged to simulate the circumstances in which a plug-in hybrid electric vehicle is used. After each month, during which the battery either experiences a small or large current ripple, characterization tests are performed to establisch the ageing of the batteries. Based on the test results, the current ripple does not appear to have a measurable impact on the battery resistance and the Discharge and Regen Power. There is an increase of the resistance and a decrease of the Discharge and Regen Power, but this is to be expected as the battery packs are submitted to 3 months of Combined Cycle Life Testing. The temperature of the battery turns out to be far more important for the resistance and attained power levels of the batteries. The absent effect of the current ripple on the ageing of the batteries may be due to the intrinsic double-layer capacitor. This capacitor at the surface of the electrodes carries part of the current ripple and reduces the current ripple as experienced by the actual charge transfer reaction which carries the dc-part of the current.

Keywords: dc-dc converter, lithium battery, PHEV (plug in hybrid electric vehicle), cycle life

1 Introduction

In this paper the impact of the current ripple originating from a bidirectional boost converter on the ageing of Li-ion batteries is investigated. This type of boost converter can be found in plug-in hybrid electric vehicles (PHEVs) and battery electric vehicles (BEVs) as it allows a wider speed range operation without early field weakening for the electric motor, while the battery voltage and number of cells can be reduced [1]. A well-known example is the Toyota Prius PHV [2]. Bidirectional boost dc-dc converters are often realised with hard-switching half-bridges in the low to medium frequency range because of their low component count, high full-load efficiency and simplicity. This leads to a low-cost, low-volume, low-weight solution for high power dc-dc converters [3]. Although only a dc-current is required to (dis)charge the battery, the operation of the converter results in the presence of a current ripple due to the

switching of the half-bridges.

The design of most bidirectional dc-dc converters developed for battery storage applications, takes the reduction of the battery current ripple into consideration. The current ripple reduction can be achieved by putting a capacitor in parallel with the battery for a single-phase dc-dc converter as described in [4] and [5]. The current ripple can be further reduced by combining a two-phase interleaved dc-dc converter with a capacitor such as proposed by [6] and [7] or even by combining a three-phase interleaved converter and a capacitor such as [8] and [9]. Soft-switching converters also rely on a capacitor to reduce the current ripple of the battery current [10], [11].

The focus is mostly put on very low (μHz) to low (Hz) frequencies, such as when the impedance is determined using electrochemical impedance spectroscopy (EIS) [12]. The choice of these frequencies is based on the discharge characteristics of the battery, e.g. the discharging of an electric vehicle does not take more than 2 hours (50 μHz) [13]. The results of these impedance measurements are used to create very accurate battery models, e.g. to estimate the State of Charge of the battery.
The Li-ion battery impedance model, as proposed by [14], is based on constant current charge and discharge pulses to predict the loaded voltage and battery SoC. The constant current pulses on which the impedance model is based last for tens of seconds, i.e. the frequency is well below 1 Hz. The model only takes the dc-value of the current into account to predict the ohmic and polarisation voltage drop and the voltage drop caused by the decrease of the battery SoC, but does not take the current ripple and its effect on the battery voltage into account.
An analytical impedance model of a Li-ion battery is proposed by [15]. The equivalent circuit of this model takes the ohmic resistance, the activation polarisation resistance, the concentration polarisation resistance and the double layer capacitance into account. The influence of the ageing of the battery on the parameters of the analytical model is investigated, but the effect of the current ripple on the ageing or the parameters of the analytical impedance model is not considered.
However, none of these models considers the effect of the current ripple on the battery, as the switching frequency of converters is in the kHz range. The applied current ripples also remain well below the expected current ripple originating from a dc-dc converter.
In [16] a multiple time-constant battery model for dynamic simulations of (hybrid) electric powertrains is introduced, using three parallel RC-branches with a time-constant of respectively seconds, minutes and hours. The resistors and capacitors of the model are function of the SOC. The model, as shown in figure 1, includes a State of Charge estimation based on charge and discharge currents with corrections for the temperature, cycle number and charge and discharge rates. Time-constants below the seconds range are not taken into account as the measured voltage drop at a switching frequency of 10 kHz does not show evidence of exponential behaviour. In this model the series resistance component $R_s(SOC)$ of the battery model is deemed sufficient to model the voltage drop corresponding to the switching frequency. The effects of the current ripple and voltage ripple on factors such as the battery life are not considered in this model, although other factors such as the cycle life, temperature and charge and discharge rate are taken into account.

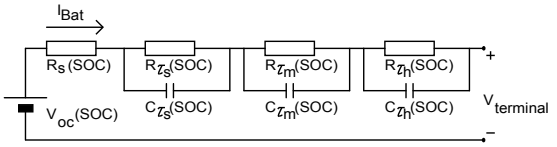

Fig. 1: Multiple time-constant battery model for dynamic electric vehicle simulations

[17] describes the dynamic properties of batteries. The electron transport in the electrodes which provides the current towards the external circuit is accompanied by ion-transport in the electrolyte. The ion-transport is largely done by diffusion. The time constants of the diffusion process depend a.o. on the electrode thickness and structure and are in the range of seconds to minutes. Another effect which has to be taken into account is the double-layer effect. A charge layer is formed between the electrode and the electrolyte. As the electrodes have a large surface and as the thickness of the charge layer is very small, the double-layer capacitance cannot be neglected. As this double-layer capacitor exists at the surface of the electrode, the current through the double-layer capacitor (C_{DL}) is in parallel with the current of the electrochemical charge transfer reaction, represented by the resistor R_{CT}. This is shown in figure 2 along with the series resistance R_s which represents the ohmic resistance of the electrolyte and current collector.

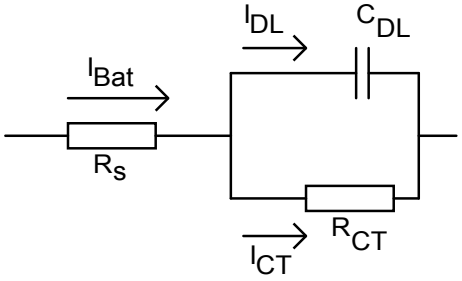

Fig. 2: Equivalent circuit of charge transfer and double-layer effects

The battery current of figure 2 is divided in two parts. At the electrode/electrolyte boundary, part of the current flows through the charge transfer reaction, while the remaining part flows through

the double-layer capacitor. Together, R_{CT} and C_{DL} acts as a low-pass filter for the charge transfer reaction. This causes the actual charge transfer reaction to carry the dc-current and a reduced current ripple, while the double-layer capacitor carries the remaining part of the current ripple. It remains unclear to which extent the current ripple originating from the dc-dc converter is flowing through this double-layer capacitor. In steady-state the dc-current entirely flows through the charge transfer reaction. The capacitance of the double-layer capacitor depends on the electrode surface, so the geometry of the battery and its electrodes are important for this value. Consequently, the geometry of the battery and its electrodes could prove to be important to divide the current ripple between the charge transfer reaction and the double-layer capacitor.

[18] introduces a high-frequency NiMH battery model to investigate the effect of the current ripple generated by the dc-dc converter. The impedance of the battery changes depending on the frequency of the current ripple. The applied current ripple covers a realistic frequency spectrum between 5 and 20 kHz and has a peak-to-peak amplitude larger than 10 A. One remarkable conclusion is that the skin effect has a measurable impact on the resistance of the battery as the frequency increases.

Although the importance of the battery current ripple reduction is acknowledged by most dc-dc converter designs, the approach is limited to the addition of a parallel capacitor and multi-phase interleaved converters. Most research focuses on frequencies and current ripples far below the switching frequencies commonly used in dc-dc converters. Only [18] discusses the skin and proximity effect at realistic switching frequencies. However, none of these discuss the effect of the current ripple on the ageing of the battery or on the operation of the battery.

In order to assess the impact of the current ripple originating from the dc-dc converter on the ageing of the battery, a set of Li-ion batteries is exposed to both small and large current ripples. To obtain a small current ripple, an LCL-filter is designed for the dc-dc converter. The LCL-filter significantly reduces the current ripple of the battery current. In order to analyse the impact of the current ripple, two identical batteries are simultaneously exposed to a different current ripple under the same circumstances during a one month period. This allows to investigate the impact of the current ripple on the discharge and regen resistance and the Discharge and Regen Power. In order to exclude any phenomena related to a single battery, the filters are switched after each month such that both batteries are exposed to small and large current ripples. First a general overview of the test set-up is given. Next, the Cycle Life Test Profile and Hybrid Pulse Power Characterization Test are briefly explained. Finally, the effect of the current ripple on the ageing of the battery is discussed.

2 General overview of test set-up

The test set-up consists of a three-phase active-front-end inverter, which is back-to-back connected to two dc-dc converters as shown in Figure 3. The switching frequency of the IGBTs in the half-bridges of the inverter and both dc-dc converters is 8 kHz. The active-front-end inverter keeps the dc-bus voltage at 650 V when the batteries are charging and discharging. Each dc-dc converter is coupled to a Li-ion battery pack. The battery pack consists of a series connection of 82 Kokam 40 Ah/3.7 V high power cells [19]. The 304 V nominal voltage, 12 kWh energy content and 28 kW power rating make this battery pack very suitable for tests such as defined by [20]. The maximum discharge current of the batteries is limited at 100 A by the dc-current capability of the dc-dc converter, while the maximum charge current of the batteries is limited at 80 A.

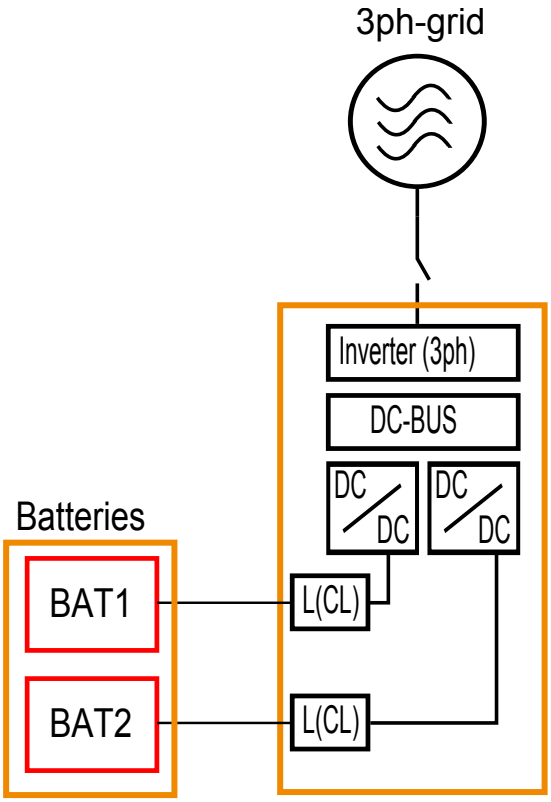

Figure 3: Overview of test set-up

The battery is equipped with a Battery Management System (BMS) that protects the individual cells against over- and undervoltages, excessive temperatures and insulation faults [21]. The voltage limit alarm is triggered when the cell voltage exceeds 4.2 V or falls below 2.9 V and shuts the converter down when activated to prevent further damage to the battery. The BMS is also equipped with cell balancing.

3 Test Cycles

The dc-dc converter can either be connected to a primary inductor of 220 μH or an LCL-filter with the same 220 μH primary inductor, a 230 μF metallized film capacitor and a 25 μH secondary inductor. The design, construction and evaluation of this filter is discussed in [22]. When the dc-dc converter is connected to the 220 μH primary inductor, the 8 kHz current ripple reaches a maximum amplitude of approximately 40 A when the battery voltage is near half of the 650 V dc-bus voltage. This set-up allows to test the impact of a large current ripple on the battery. When the dc-dc converter is connected to the mentioned LCL-filter, the current ripple amplitude is reduced below 1 A. The structure of the bidirectional boost converter and LCL-filter is shown in Figure 4, along with the current conventions of the LCL-filter.

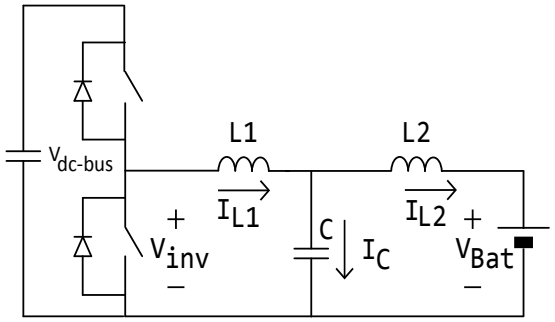

Figure 4: Dc-dc converter with LCL filter

The test profiles and characterization tests described in this paper are adopted from the *Battery Test Manual For Plug-In Hybrid Electric Vehicles* as formulated by the *United States Department of Energy (DOE), Office of Energy Efficiency and Renewable Energy (EERE), Vehicle Technologies Program* [20].

The Combined Cycle Life Test for the Maximum PHEV Battery are applied to the battery during the span of an entire month. These tests are meant to simulate the circumstances in which a plug-in hybrid vehicle is normally used. The Charge-Depleting (CD) Cycle Life Test simulates the discharging of the battery during pure electric driving. This 6-minute test profile is applied as required, but for the two 2-second bursts at 238 and 330 s, because the power has to be limited to 28 kW to take the 100 A maximum current rating of the dc-dc converter into account. The battery pack voltage is limited to 324 V to take the voltage unbalance of the cells into account. This means that the upper 7 Ah of the 40 Ah battery are not used. The lower 10 Ah of the 40 Ah battery are not used either to prevent damage by over-discharging and premature ageing. The remaining 23 Ah correspond to an energy-content of 7 kWh. The test should be performed with an energy margin of 30%, reducing the usable energy content to 4.9 kWh, such that the same number of test profiles can be used throughout the entire test period. This results in 11 consecutive CD Cycle Life Test Profiles which will be applied to discharge the battery. The applied number of test profiles is approximately half of the number prescribed by the Maximum PHEV Battery Target, but this is necessary to prevent damage to the battery. This test sequence is followed by the Charge-Sustaining (CS) Cycle Life Test, simulating the charging and discharging of the battery during hybrid driving mode. The profile lasts 90 s and imposes a 50 Wh swing assuming 90 % battery efficiency, i.e. the profile removes 50 Wh but recharges the battery pack with 56.3 Wh to compensate for the losses of the battery. This profile can be implemented without adaptation. As the number of CS Cycle Life Test Profiles is 3 times the number of CD Cycle Life Test Profiles, this profile is repeated 33 times. This results in a Combined Cycle Life Test of 115.5 minutes. In between the CD and CS Cycle Life Test and the recharging of the batteries (and vice versa), a one-hour rest period is applied to bring the battery pack in electrochemical and thermal equilibrium. The batteries are subsequently charged to the predefined charge voltage at a charge current of 4 A.

The Combined Cycle Life Test is repeated continuously for 28 days. After this period the degradation of the battery pack under test is established by performing the Hybrid Pulse Power Characterization Test (HPPC-Test). These tests are performed prior to the beginning of the Combined Cycle Life Tests and after each interval of 28 days. The HPPC-Test is intended to determine the dynamic power capability over the battery's useable voltage range. The objective of this test is to establish, as a function of depth-of-discharge, the discharge power capability at the end of a 10-s 100 A discharge current pulse and regenerative power capability at the end of a 10-s 75 A regenerative current pulse. The HPPC-Test Profile is shown in figure 5 and measures the resistance across the voltage range of the battery during discharging and regenerative braking. After each HPPC-Test a further 10 % DOD is removed from the battery, followed by a 1 hour rest period. This is repeated across the entire DOD range of the battery. The Discharge and Regen Pulse Power Capability is calculated at each available DOD increment from the open-circuit voltage (OCV) and the resistance determined for that DOD, thus allowing to determine the ageing of the battery after each month of testing.

In the first month of the cycle life tests, the first battery pack is exposed to the current ripple of the 220 μH primary inductor, while the second battery pack is exposed to the current ripple of the LCL-filter with 220 μH primary inductor, 230 μF capacitor and 25 μH secondary inductor. This results in a current ripple of approximately 75 A_{pp} for the first battery pack and approximately 2 A_{pp} for the second battery pack. In the second month of the tests, the filters are switched, such that the first battery pack is exposed to the very small current ripple and the second battery pack to the very large

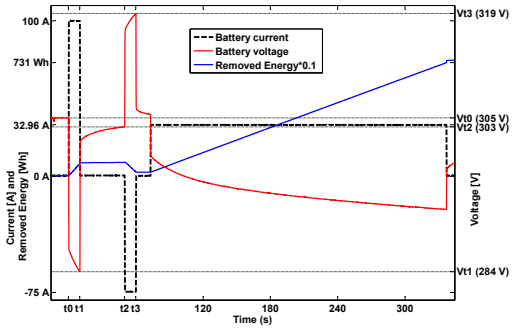

Fig. 5: Example of HPPC-test-pulse at 50 % DOD, followed by 10 % depth of discharge increment.

current ripple. In the third month of the tests, both batteries are connected to the described LCL-filter, i.e. both experience only a very small current ripple.

4 Test Results

4.1 Evolution of the discharge and regen resistance

The data collected by the HPPC-Test at 10% DOD increments is used to calculate the resistance of the battery pack during discharging and regenerative charging. The discharge and regen resistance are calculated using equation 1 and 2 respectively. The voltages are shown on the second y-axis in figure 5, the currents refer to the 100 A current pulse for the discharge resistance and the -75 A current pulse for the regen resistance shown in figure 5.

$$R_{discharge} = \frac{\Delta V_{discharge}}{\Delta I_{discharge}} = \left| \frac{V_{t1} - V_{t0}}{I_{t1} - I_{t0}} \right| \ [m\Omega] \quad (1)$$

$$R_{regen} = \frac{\Delta V_{regen}}{\Delta I_{regen}} = \left| \frac{V_{t3} - V_{t2}}{I_{t3} - I_{t2}} \right| \ [m\Omega] \quad (2)$$

The resistance of the battery packs prior to the cycle life test and after each month of testing is shown in figure 6 for the first battery pack and figure 7 for the second battery pack.
The initial discharge and regen resistance of the first battery pack is between 178 and 204 $m\Omega$. After being exposed to the large 75 A current ripple for one month, both resistances increase significantly to a level between 205 and 221 $m\Omega$. Initially, the discharge and regen resistances of the second battery pack are between 178 and 199 $m\Omega$. After one month of cycle life testing at a very small current ripple, both resistances remained approximately the same up to 40 % DOD, at 50 % DOD and beyond both resistances increased, but never more than 10 $m\Omega$ compared to the initial value.

In the second month, the second battery pack is exposed to the large 75 A current ripple, while the first battery pack is exposed to a very small current ripple as it is connected to the LCL-filter. In both cases the resistance of the battery pack increases across the whole DOD range. The discharge and charge resistance of the first battery pack increase between 25 and 35 $m\Omega$. In the case of the second battery pack the discharge and charge resistance increase between 13 and 18 $m\Omega$, not taking the resistance at 80 and 90% DOD into account.
In the third month both battery packs are connected to identical LCL-filters, so neither is exposed to a large current ripple. The regen and discharge resistance of the first battery pack decrease between 20 and 37 $m\Omega$, while the resistances of the second battery pack decrease between 7 and 14 $m\Omega$. This brings the resistances of both battery packs back to the level of the first month.

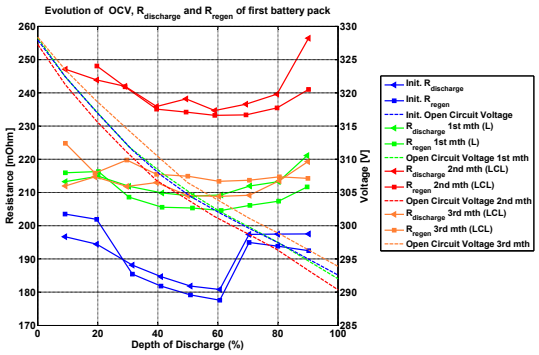

Fig. 6: Evolution of Open Circuit Voltage, discharge and regen resistance of first battery pack.

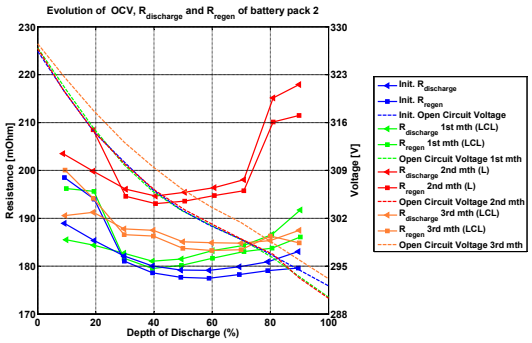

Fig. 7: Evolution of Open Circuit Voltage, discharge and regen resistance of second battery pack.

Although the results after the first month of testing might suggest that the current ripple is responsible for the increase of the resistance (i.e. both discharge and charge resistance) of the first battery pack while the second battery pack is less affected, both battery packs will see a sharp increase of the resistance in the

second month of testing. Besides the expected increase of resistance due to the ageing of the batteries, most probably the temperature of the battery is far more important for the resistance of the batteries. During the measurement of the HPPC-Test prior to and after one month of testing, the battery temperature is slightly above 20°C, while the battery temperature during the measurement of the HPPC-Test after 2 months of testing was below 20°C. The increase of the resistance of the first battery pack after one month of testing is also related to the increased voltage unbalance of the battery pack [23], but this is beyond the scope of this paper. As both batteries are colder, the measured resistance increases after the second month. During the measurement of the HPPC-Test after the third month of testing the battery temperature was around 25°C. This caused the resistance of both batteries to decrease significantly in comparison with the second month. Clearly, the battery temperature has the most dominant influence on the battery resistance. When the battery temperature is lower, both battery packs experience a sharp increase of the resistance, while the resistance is far lower when the battery temperature increases. Based on these results, the current ripple does not appear to have a measurable impact on the battery resistance. There is an increase of the battery resistance, but this is to be expected as the battery packs are submitted to 3 months of Combined Cycle Life Testing.

4.2 Evolution of the Discharge and Regen peak power and the Charge-Sustaining Available Energy

Given the discharge and regen resistances together with the OCV as function of the DOD, the discharge and regen 10 s-peak powers can be calculated using equations 3 and 4 [20].

$$Discharge\ Pulse\ Power\ Capability = \frac{V_{\min} \cdot (OCV_{dis} - V_{\min})}{R_{discharge}}\ [W] \quad (3)$$

$$Regen\ Pulse\ Power\ Capability = \frac{V_{\max} \cdot (V_{\max} - OCV_{regen})}{R_{regen}}\ [W] \quad (4)$$

In these equations, the minimum and maximum voltages are equal to 3.05 and 4.15 V respectively per cell. This corresponds with a minimum and maximum voltage of 250 and 340 V respectively at battery pack level. The resulting discharge and regen 10 s-peak powers are shown in figure 8 and 9. The Charge Sustaining (CS) Available Energy is defined as the energy removed during a 10-kW discharge over the DOD range for which the Discharge Power Target, 60 kW in this case, and the Regen Power Target, 40 kW, are precisely met. The Regen Power Target is two thirds of the discharge power and is plotted on a second y-axis, as prescribed by the manual [20]. The 60 kW Discharge Power Target is a realistic value for the peak power, as this results in a battery current of 240 A at 250 V, which is below the peak current of 400 A which the battery is able to deliver. The 40 kW Regen Power Target has to be considered as a theoritical value based on the maximum voltage of 340 V and the regen resistance of the battery, but which is certainly not recommended in practice, as the charge current would be approximately 145 A at low voltages, which is above the 80 A maximum charge current.

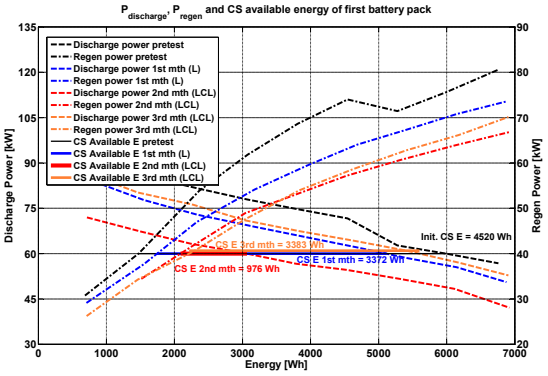

Fig. 8: Evolution of discharge and regen power of first battery pack

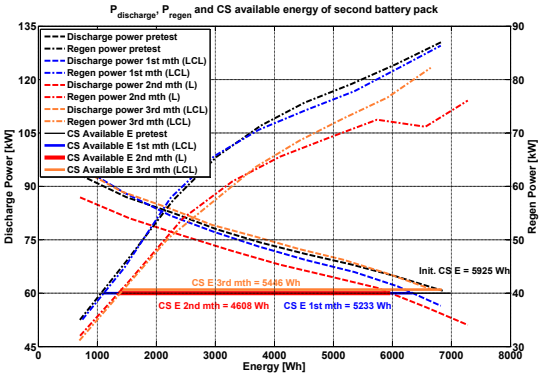

Fig. 9: Evolution of discharge and regen power of second battery pack

The Discharge and Regen Power of the first battery pack decrease notably after the first and second month of testing. After the third month, the Discharge Power is slightly higher than the level attained after the first month, while the Regen Power remains at the level of the second month. As explained, the Discharge and Regen Power decrease in the second month due to the lower temperature of the battery. After the third month neither of them decreases because the battery temperature is higher. The decrease of

the Discharge Power has serious consequences on the Charge Sustaining Available Energy. After the first month, the CS Available Energy drops from 4.5 kWh to 3.4 kWh. After the second month and given the sharp decrease in both Discharge and Regen Power, the CS Available Energy drops to less than 1 kWh. After the third month, the CS Available Energy will increase sharply to 3.4 kWh, as the Discharge Power is much higher than after the second month. The impact of the Regen Power on the CS Available Energy is much lower and is only reponsible for the loss of some 0.5 kWh of CS Available Energy in three months of testing.

In the case of the second battery pack, on which only a small current ripple is imposed in the first month, the Discharge and Regen Power slightly decrease. In the second month, the Discharge Power decreases some 5 kW, while the Regen Power decreases even more, specially at the higher DOD-range. This corresponds with the results of the first battery. The decrease of the Discharge and Regen Power observed in both batteries cannot be explained by the current ripple, as the second battery pack is subjected to the large ripple and the first pack to the small ripple. However, the decrease can be explained when the lowered temperature of both packs during the HPPC-Test is taken into account. This explanation remains valid after the third month of testing. Here, the Regen Power remains at the level of the second month for both batteries. The Discharge Power increases to a level slightly above the level from the HPPC-Test after the second month. Again, these results cannot be explained by the current ripple (small in both cases), as the current ripple cannot cause an increase of the Discharge Power. However, the temperature can cause the Discharge Power to increase, as the resistance of the battery is lower at elevated temperatures. The CS Available Energy of the second battery pack decreases from 5.9 kWh over 5.2 kWh to 4.6 kWh after the first and second month of testing. After the third month, the CS Available Energy increases to 5.4 kWh.

5 Conclusions

This work investigates the effect of the current ripple originating from the dc-dc converter on the ageing of Li-ion batteries. For this purpose a test set-up is build with two bidirectional dc-dc converters connected to two identical 12 kWh/28 kW Li-ion batteries. In order to attain different current ripples with this set-up, an LCL-filter is designed which in practice achieves an almost complete elimination of the battery current ripple. When the battery is solely connected to the primary inductor of this filter, the battery is exposed to a large current ripple. In order to assess the impact of the current ripple on the ageing of the battery, both battery packs are exposed to the Combined Cycle Life Tests during three months. During each test period of one month the battery is either subjected to a high or low current ripple. At the end of each one month test period the degradation of the battery is measured by performing the HPPC-Test.

The results of these test show that both batteries age during the three month test period, resulting in an increase of the discharge and regen resistance. However, the ageing cannot be linked to the applied current ripple. The temperature of the battery at the moment of the resistance measurements proves to be far more important. Both batteries experience a significant increase of the battery resistance when the temperature is lower and a decrease when the temperature is higher, likewise both batteries experience a significant decrease of the Discharge and Regen Power when the temperature is lower and an increase when the temperature is higher. The fade of the CS Available Energy of both battery packs also clearly supports that the current ripple is not responsible for the ageing of the battery.

The intrinsic double-layer capacitor at the surface of the electrodes offers an explanation for the lack of impact of the battery current ripple on the ageing of the battery. This capacitor is able to carry part of the current ripple, effectively reducing the current ripple as experienced by the charge transfer reaction. This also implies that the design of future batteries might benefit from taking the double-layer capacitance into account, as this could influence the ageing of the battery. A second implication is that this research reveals the need for a high frequency battery model. This will become increasingly important, given the trends towards new switches such as GaN which will impose a current ripple with a frequency in the hundreds of kHz on the battery.

References

[1] J.-S. J. Lai and D. J. Nelson, "Energy Management Power Converters in Hybrid Electric and Fuel Cell Vehicles," *Proceedings of the IEEE*, vol. 95, no. 4, pp. 766–777, April 2007.

[2] (2011, November) Toyota starts taking orders for soon-to-be-launched Prius PHV plug-in hybrid in Japan. Toyota Motor Company. [Online]. Available: http://www.greencarcongress.com/2011

[3] B. J. Lyons, J. G. Hayes, and M. G. Egan, "Magnetic Material Comparisons for High-Current Inductors in Low-Medium Frequency dc-dc Converters," *Applied Power Electronics Conference (APEC)*, vol. 1, pp. 71–77, 2007.

[4] W. Lee, B.-M. Han, and H. Cha, "Battery Ripple Current Reduction in a Three-phase Interleaved dc-dc Converter for 5kW Battery Charger,"

IEEE Energy Conversion Congress and Exposition (ECCE), pp. 3535 – 3540, 2011.

[5] T. A. Burress, C. L. Coomer, S. L. Campbell, L. E. Seiber, L. D. Marlino, R. H. Staunton, and J. P. Cunningham, "Evaluation of the 2007 Toyota Camry Hybrid Synergy Drive System," Oak Ridge National Laboratory, Engineering Science and Technology Division, Tech. Rep., April 2008.

[6] X. Huang, X. Wang, T. Nergaard, J. Lai, X. Xu, and L. Zhu, "Parasitic Ringing and Design Issues of Digitally Controlled High Power Interleaved Boost Converters," *IEEE Transactions on Power Electronics*, vol. 19, no. 5, pp. 1341–1352, September 2004.

[7] P. James, A. Forsyth, G. Calderon-Lopez, and P. V., "Dc-dc converter for Hybrid and All Electric Vehicles," *Electric Vehicle Symposium (EVS24)*, p. 9 pages, May 2009.

[8] J. Zhang, J.-S. Lai, R.-Y. Kim, and W. Yu, "High-Power Density Design of a Soft-Switching High-Power Bidirectional dc-dc Converter," *IEEE Transactions on Power Electronics*, vol. 22, no. 4, pp. 1145–1153, July 2007.

[9] D. Urciuoli and C. Tipton, "Development of a 90 kW Bidirectional dc-dc Converter for Power Dense Applications," *Twenty-First Annual IEEE Applied Power Electronics Conference and Exposition*, pp. 1375–1378, March 2006.

[10] S. Waffler and J. Kolar, "Comparative Evaluation of Soft-Switching Concepts for Bidirectional Buck and Boost dc-dc Converters," *International Power Electronics Conference*, vol. 1856-1865, p. 6, 2010.

[11] M. Pavlovsky, Y. Tsuruta, and A. Kawamura, "Recent Improvements of Efficiency and Power Density of dc-dc Converters for Automotive Applications," *International Power Electronics Conference*, pp. 1866–1873, 2010.

[12] S. Buller, M. Thele, R. De Doncker, and E. Karden, "Impedance-Based Simulation Models of Supercapacitors and Li-ion Batteries for Power Electronic Applications," *IEEE Transactions on Industry Applications*, pp. 742 – 747, 2005.

[13] P. Mauracher and E. Karden, "Dynamic Modelling of Lead-acid Batteries using Impedance Spectroscopy for Parameter Identification," *Journal of Power Sources: Proceedings of the Fifth European Lead Battery Conference*, vol. 67, p. 6984, 1997.

[14] M. Zheng, B. Qi, and X. Du, "Dynamic Model for Characteristics of Li-ion Battery on Electric Vehicle," *4th IEEE Conference on Industrial Electronics and Applications*, pp. 2867 – 2871, 2009.

[15] W. Luo, C. Lv, L. Wang, and C. Liu, "Study on Impedance Model of Li-ion Battery," *6th IEEE Conference on Industrial Electronics and Applications (ICIEA)*, pp. 1943 – 1947, 2011.

[16] R. Kroeze and P. Krein, "Electrical Battery Model for Use in Dynamic Electric Vehicle Simulations," in *IEEE Power Electronics Specialists Conference (PESC)*, june 2008, pp. 1336 –1342.

[17] A. Jossen, "Fundamentals of Battery Dynamics," in *Journal of Power Sources 154*, E. BV, Ed., 2006, pp. 530–538.

[18] J. Wang, K. Zou, C. Chen, and L. Chen, "A High Frequency Battery Model for Current Ripple Analysis," *Applied Power Electronics Conference and Exposition (APEC)*, pp. 676 – 680, 2010.

[19] *Technical Specificaton SLPB100216216H*, Kokam, March 23 2009.

[20] Idaho National Laboratory, *Battery Test Manual for Plug-In Hybrid Electric Vehicles*, United States Department of Energy (DOE), Office of Energy Efficiency and Renewable Energy (EERE), Vehicle Technologies Program, March 2008.

[21] D. Andrea, *Battery Management Systems for Large Lithium Ion Battery Packs*. Artech House, 2010.

[22] S. De Breucker, R. D'hulst, and J. Driesen, "Design of dc-dc converters with LCL-filters: Impact on Battery and Battery Management System," *European Electric Vehicle Congress (EEVC) 2012, Brussels, Belgium*, pp. 1–12, 19-22 November 2012.

[23] S. De Breucker, "Impact of dc-dc Converters on Li-ion Batteries," Ph.D. dissertation, Arenberg Doctoral School Wetenschap & Technologie, 2012.

Authors

Sven De Breucker was born in 1980 in Belgium. He received the M.Eng. degree in Electromechanics in 2002 from the De Nayer College University, the M.Sc. degree in Electrotechnical Engineering in 2005 from the KULeuven (Catholic University of Leuven), Belgium and his Ph.D. in Electrotechnical Engineering in 2012. He currently works as a researcher at the unit Energy Technology (ETE) of VITO (Flemish Institute for Technological Research). His main interests are (control of) power electronics and plug-in hybrid electric vehicles. His research focuses on dc-dc converters, batteries and grid-coupled inverters.

Kristof Engelen received the M.Sc. degree in electrical engineering from Katholieke Universiteit Leuven (KU Leuven), Leuven, Belgium, in 2005. He is currently a Research Assistant at K.U. Leuven ESAT/ELECTA, where he is working toward the Ph.D. degree. His research interests include power electronics and its applications.

Reinhilde D'hulst graduated in 2004 as M.Sc. in Electrical Engineering from the Katholieke Universiteit Leuven (KU Leuven). She obtained her Ph.D. in Electrical Engineering from the K.U.Leuven in 2009 after working on power management circuits for energy harvesters. Currently she works for VITO, the Flemisch Institute for Technological Research where she is involved in several research projects related to Smart Grids. She does research on grid- connecting issues of renewable energy resources and control algorithms for Demand Side Management.

Johan Driesen (S'93-M'97) was born in 1973 in Belgium. He received the M.Sc. degree in 1996 as Electrotechnical Engineer from the K.U.Leuven, Belgium. He received the Ph.D. degree in Electrical Engineering at K.U.Leuven in 2000 on the finite element solution of coupled thermal-electromagnetic problems and related applications in electrical machines and drives, microsystems and power quality issues. Currently he is a professor at the K.U.Leuven and teaches power electronics and drives. In 2000-2001 he was a visiting researcher in the Imperial College of Science, Technology and Medicine, London, UK. In 2002 he was working at the University of California, Berkeley, USA. Currently he conducts research on distributed generation, including renewable energy systems, power electronics and its applications, for instance in drives and power quality.